Supplementary information: Machine learning to support visual auditing of home-based lateral flow immunoassay self-test results for SARS-CoV-2 antibodies

Supplementary Information 3 – Blood leakage anomaly detection

Figure S3-1: Ensemble averages for different user-reported test-result-conditions

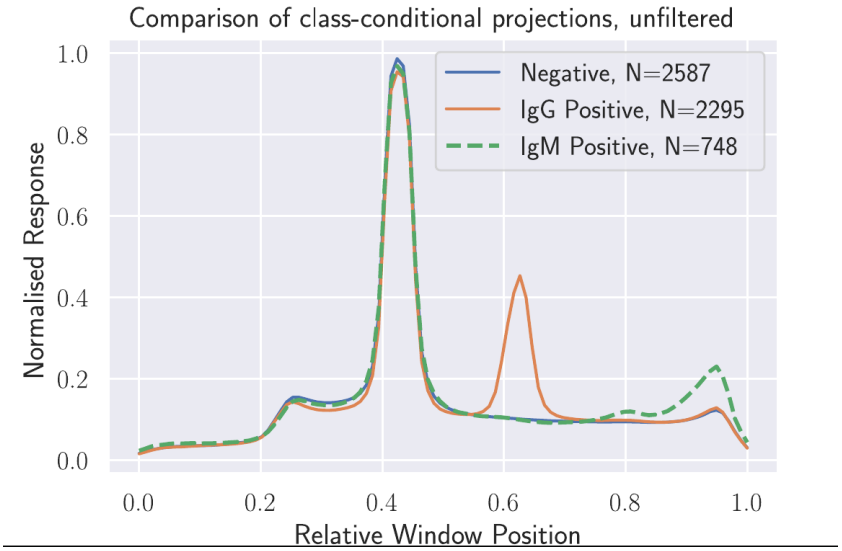


Figure S3-2: Examples of broken devices (a) "heavy" (b) and "light" (c) blood leakage

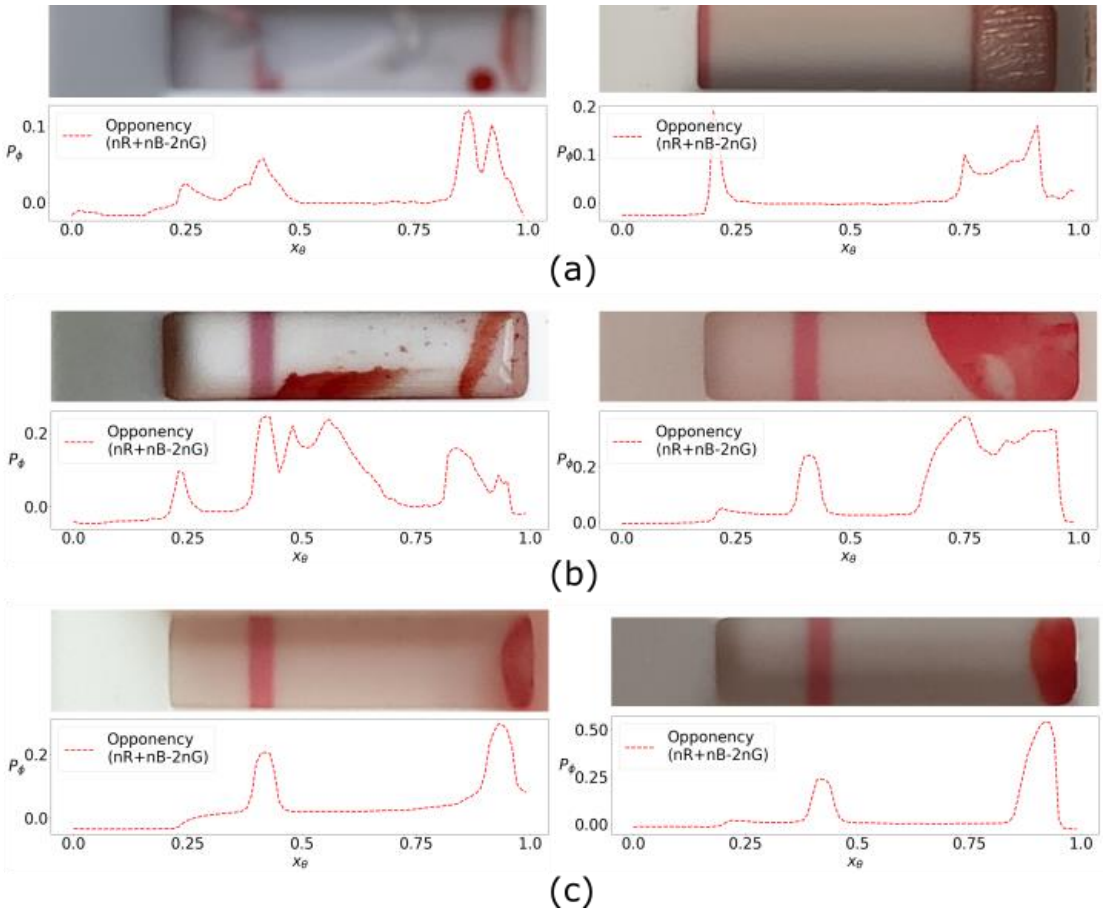
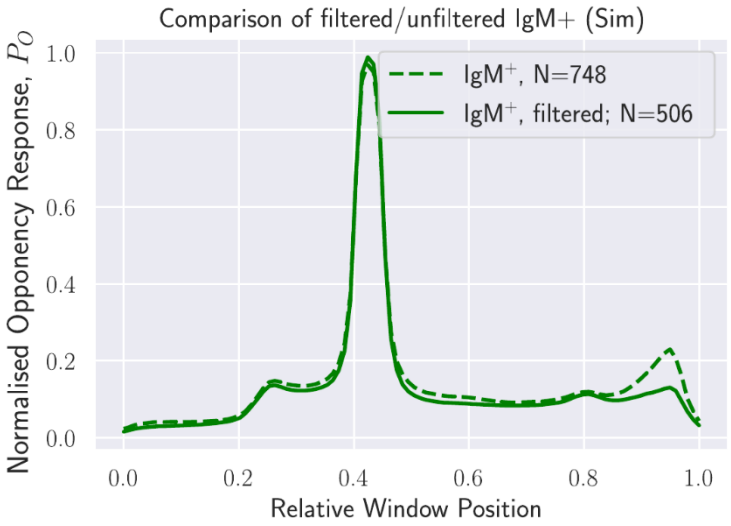


Figure S3-3: Difference between filtered and unfiltered IgM ensemble signatures



Appendix S3-A - Anomaly Detection

The opponency projection signature was found to be a good proxy for two-dimensional interpretation of the test window. Though it does not capture intensity variations that are parallel to the lines of the assay, it enables semi-quantitative analyses through alignment and ensemble-averaging of the signals. By grouping, aligning, and ensemble-averaging the projection signatures corresponding to different user-reported results, we observed an elevated region of the signature in users who self-reported as being IgM positive (Figure S3-1, green). This region was not at the expected location for the IgM line, but rather toward the edge of the read-out window. Closer scrutiny revealed that many self-reported IgM positive cases were due to leakage of the blood sample into the read-out window in such a way as to produce a clear (and thin) red line. Training a system to detect blood leakage – as well as broken devices – would be a natural next step, but variations in details of blood-leakage and spoiled tests vary dramatically and can be difficult to find in a large corpus of images. Observing the high degree of clustering of opponency signals around positive and negative cases (Figure S3-1, blue and orange), we used two simple measures for anomaly detection, both based on comparisons between a template signal and the fixed length (100 spatial samples) opponency signal obtained from the read-out window of a specific image, $P_O^{(i)}(n), n = 0,1,2, \ldots 99$ (see Supplementary Information 1 Appendix S1-D). The comparisons are based on normalised cross-correlation between the template signal and a candidate opponency signal:

$$\rho^{(i)}(k) = \langle \mu(n)/\|\mu(n)\| \, , P_O^{(i)}(n+k) \, / \left\| P_O^{(i)}(n) \right\| \rangle$$

and anomalies are flagged under either of two conditions:

$$\arg\max[\rho^{(i)}(k)] > \eta/2$$

and

$$\max[\rho^{(i)}(k)] < \gamma$$

The template signal is defined by $\mu(n) = \mathbb{E}[P_O(n)]$, where the expectation, $\mathbb{E}$, is taken over a sufficiently large ensemble of projection signals drawn at random from all classes. We found little

change in the shape of the template, $\mu(n)$, beyond a sample size of 5,000 signals. The value of η is set to be 1/3 of the length of the read-out window, since shifts of both IgG positive and negative projections were very unlikely to be outside of this range; the value of γ (a cosine similarity measure, $0 \leq |\gamma| \leq 1$) is close to 1 for most sample classes; we found (empirically) that setting a value of 0.85 provided a good filter for unusual projection signatures in a manner that was uncorrelated with expertly-determined IgG status.

Anomalies detected by either of these two conditions are flagged for expert human review; a sample of the read-out windows containing such cases is shown in Figure S3-2. After such anomalies are removed through filtering, the elevated section of the opponency signature – and therefore user-reported false positives – is significantly reduced, leaving us with a higher proportion of true, user-reported IgM positives (Figure S3-3).